 CMC, vol.26, no.1, pp.1-17, 2011

A Modified Prandtl-Ishlinskii Model and its Applications to Inverse Control of Piezoelectric Actuators

J. H. Qiu[1,2], H. Jiang[1], H. L. Ji[1] and N. Hu[3]

Abstract: Piezoelectric actuators based motion-producing devices are widely used in precision machining, deformable mirrors, micropumps and piezoelectric injection systems. However, because of their hysteresis nonlinear property, the piezoelectric actuators can not provide absolutely precise displacements. To solve this problem, researchers applied inverse control method to compensate the nonlinearity of piezoelectric actuators, and the inverse models are mainly based on traditional hysteresis models such as the Preiasch model or Prandtl-Ishlinskii model. In this paper, a new approach for inverse control of piezoelectric actuators is presented. The new method utilize a modified Prandtl-Ishlinskii model which is based on a combination of two asymmetric hysteresis operators, and the two operators can independently model ascending branches and descending branches of hysteresis loops. Based on the inversion of the proposed model, an open-loop inverse controller and an adaptive inverse controller are designed and implemented in a real-time control system. The performances of the two controllers are tested and assessed. The experimental results show that the open-loop inverse controller can suppress the hysteresis nonlinearity to 2.31% and the adaptive inverse controller can reduce the hysteresis nonlinearity to 2.02%.

Keywords: piezoelectric actuators, inverse control, modified Prandtl-Ishlinskii model

1 Introduction

Piezoelectric actuators are widely used in micro-positioning devices as they can generate displacement with sub-nanometer level resolution. However, due to the intrinsic ferroelectricity of piezoceramics, hysteretic nonlinearities are present in

[1] State Key Laboratory of Mechanics and Control of Mechanical Structures, Nanjing University of Aeronautics and Astronautics, Nanjing, China
[2] Corresponding author: Tel: (86) 2584891123; Fax: (86) 2584891123; E-mail: qiu@nuaa.edu.cn
[3] Chiba University, Chiba, Japan

piezoelectric actuators and their positioning accuracy is greatly affected. In order to compensate the hysteresis nonlinearity of piezoelectric actuators, a lot of methods have been developed and they can be briefly classified into three categories: electric charge control, closed-loop control and open-loop inverse control [Newcomb and Flinn (1982); Furutani *et al.* (1998); Barrett and Quate (1991); Croft *et al.* (1999)]. The open-loop inverse control utilizes an inverse hysteresis model to compensate the nonlinearity of a piezoelectric actuator. This scheme requires precise mathematical model that closely describes hysteresis behavior of actuators but doesn't need any position sensor, and the control system is immune to instability problem. Therefore, inverse model based compensation has become a more attractive option in some tracking control applications.

The Preisach model [Ge and Jouaneh (1995); Ge and Jouanen (1996); Hughes and Wen (1997); Hu and Mrad (2002)] is a well-known hysteresis model that has been proposed and developed for hysteresis modeling and compensation. Besides, the Generalized Maxwell Slip (GMS) model [Goldfarb and Celanovic (1997); Badel *et al.* (2007)] and the Prandtl-Ishlinskii model [Janocha and Kuhnen (2000); Janaideh *et al.* (2008)] have also been used in hysteresis modeling of piezoelectric actuators. The Preisach model can model various types of hysteresis loops, but it requires plenty of parameters and costs a lot of computation to identify those parameters. In contrast, the Prandtl-Ishlinskii model and GMS model are analytically invertible, much simpler than the Preisach model, and can easily be used to design inverse controller. Both of the two models have an odd symmetry property so that they can only model centrally symmetric hysteresis loops. However, the hysteresis loops of most piezoelectric actuators are not centrally symmetric [Miller and Savage (1959)]. To overcome the odd symmetry property, the Prandtl-Ishlinskii operator is combined with a saturation operator in series and nonsymmetrical nonlinearity is added to the classical Prandtl-Ishlinskii operator. This approach allows modeling of asymmetric hysteresis loops, but it also features twice transformation of input signals therefore increases the complexity and computation cost of parameter identification [Kuhnen (2003); Ang *et al.* (2007)].

In the former study a modified Prandtl-Ishlinskii model is proposed for modeling nonsymmetrical hysteresis nonlinearity of piezoelectric actuators [Jiang *et al.* (2009)]. This approach overcomes the odd symmetry restrictive by combining two asymmetric operators in parallel, and the two asymmetric operators respectively correspond to the ascending branch and the descend branch of a complete hysteresis loop. It was proved that the proposed model satisfies wiping-out property but does not satisfy congruency property. The identification of the proposed model was based on an recursive least-square method, and this is a main advantage of the proposed model because the identification procedure is faster and simpler than the

identification procedures of other classical hysteresis models. The proposed model also exhibited a very high accuracy in characterizing the hysteresis nonlinearity of piezoelectric actuators.

In this study, the modified Prandtl-Ishlinskii model is applied to the inverse control of hysteresis of a piezoelectric actuator to validate its effectiveness. Two controllers based on the inverse model of the modified Prandtl-Ishlinskii model, one feedforward inverse controller and the other an adaptive inverse controller, are developed. Both the two controllers are implemented in real-time control tasks and experimental results show that the inverse modified Prandtl-Ishlinskii model-based controller is effective for hysteresis compensation of piezoelectric actuators.

2 The Inverse Modified Prandtl-Ishlinskii Model

Because the classical Prandtl-Ishlinskii model can not characterize the asymmetric hysteresis of piezoelectric actuators, a modified Prandtl-Ishlinskii model for asymmetric hysteretic nonlinearity of piezoelectric actuators was proposed in the former study [Jiang *et al.* (2009)]. The proposed asymmetric play operator consists of two parts, which are called the right-side play operator (RSPO) and the left-side play operator (LSPO). They respectively represent the right-side hysteretic nonlinearity and the left-side hysteretic nonlinearity of a system with hysteresis. The Prandtl-Ishlinskii inverse model is based on the inverse operator of RSPO and LSPO. In order to drive the inverse model, the modified Prandtl-Ishlinskii model is introduced first.

2.1 The modified Prandtl-Ishlinskii model

If a threshold $0 < r < 1$ is given, the right-side play operator $w = F_r^r[v](t)$ for any piecewise monotone input function $v : [0, t_E] \to [0, 1]$ is define as [Jiang *et al.* (2009)]

$$\begin{aligned} w(0) &= F_r^r[v](0) = f_r^r(v(0), 0, 1, 0), \\ w(t) &= F_r^r[v](t) = f_r^r(v(t), w(t_i), \kappa(t), \lambda(t)), \quad \text{for } t_i < t < t_{i+1},\ 0 \le i < N, \end{aligned} \tag{1}$$

where

$$f_r^r(v, w, \kappa, \lambda) = \max\{\frac{v-r}{1-r}, \min\{\kappa v + \lambda, w\}\}, \tag{2}$$

$$\kappa(t) = \frac{w_M(t) - w_m(t)}{v_M(t) - v_m(t)}, \quad \lambda(t) = \frac{v_M(t)w_m(t) - v_m(t)w_M(t)}{v_M(t) - v_m(t)}, \tag{3}$$

and $v_M(t), v_m(t), w_M(t)$ and $w_m(t)$ are values related to the latest dominant extrema of $v(t)$ and $w(t)$. The dominant extrema of an input or an output string are such ex-

trema that have influences on the memory of hysteresis, and they can be generated by Madelung deletion rule [Brokate and Kenmochi (1996)].

When the threshold $0 < r < 1$ is given, the left side play operator $w = F_r^l[v](t)$ for any piecewise monotone input function $v : [0, t_E] \to R$ is define as

$$\begin{aligned} w(0) &= F_r^l[v](0) = f_r^l(v(0), 0, 1, 0), \\ w(t) &= F_r^l[v](t) = f_r^l(v(t), w(t_i), \kappa(t), \lambda(t)), \quad \text{for } t_i < t < t_{i+1},\ 0 \le i \le N-1, \end{aligned} \tag{4}$$

where

$$f_r^l(v, w, \kappa, \lambda) = \max\{\frac{v}{1-r}, \min\{\kappa v + \lambda, w\}\}, \tag{5}$$

and $\kappa(t)$ and $\lambda(t)$ are defined using the definitions given in Eq. (3). The transfer characteristics of the above two operators are shown in Figure 1, and it can be clearly seen that both RSPO and LSPO have an asymmetric transfer characteristic.

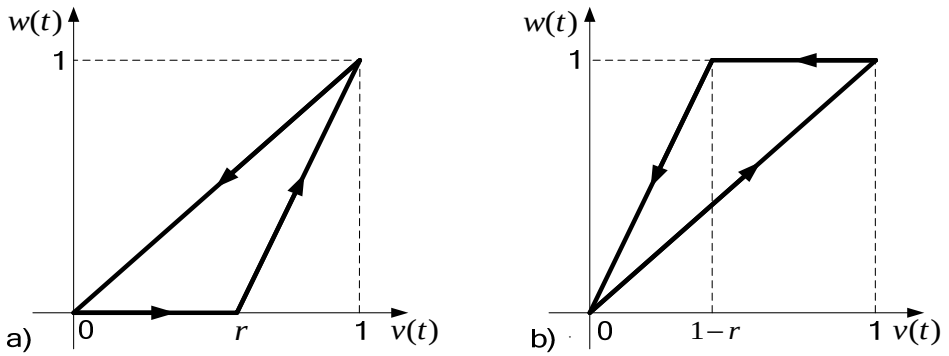

Figure 1: The transfer characteristic of an RSPO and LSPO

The modified Prandtl-Ishlinskii model is define as

$$x(t) = H[v](t) = pv(t) + \int_0^R q^r(r) F_r^r[v](t)dr + \int_0^R q^l(r) F_r^l[v](t)dr \tag{6}$$

where $q^r(r)$ and $q^l(r)$ are density functions and R is the upper limit of r. p is a constant that satisfies

$$p = \left(1 - \int_0^R q^r(r)dr - \int_0^R q^l(r)dr\right). \tag{7}$$

Substitution of Eq. (10) into Eq. (9) gives

$$x(t) = H[v](t) = v(t) + \int_0^R q^r(r)\,(F_r^r[v](t) - v(t))dr + \int_0^R q^l(r)\left(F_r^l[v](t) - v(t)\right)dr. \tag{8}$$

The discrete form of the modified Prandtl-Ishlinskii model is given by

$$x(t) = H[v](t) = v(t) + \sum_{j=1}^{M} q_j^r\left(F_{r_j}^r[v](t) - v(t)\right) + \sum_{j=1}^{M} q_j^l\left(F_{r_j}^l[v](t) - v(t)\right). \tag{9}$$

where M is the number of LSPOs or RSPOs used in the discrete modified Prandtl-Ishlinskii model.

2.2 The inverse modified Prandtl-Ishlinskii model

The inversion of the play operator-based Prandtl-Ishlinskii model is usually expressed by summation of stop operators, which are complementary of play operators. The modified Prandtl-Ishlinskii model proposed in the former study is based on RSPOs and LSPOs. In order to construct the inversion of the modified Prandtl-Ishlinskii model, right-side stop operators (RSSOs) and left-side stop operators (LSSOs) are defined as follows:

$$\begin{aligned} w(t) &= E_r^r[v](t) \\ &= \frac{v(t)}{r} - \frac{F_r^l[v](t)(1-r)}{r} \\ &= \frac{v(t)}{r} - \min\left\{\frac{v(t)}{r}, \frac{1-r}{r}\min\left\{\kappa v(t) + \lambda, w(t_i)\right\}\right\} \quad (t_i < t \le t_{i+1}) \end{aligned} \tag{10}$$

and

$$\begin{aligned} w(t) &= E_r^l[v](t) \\ &= \frac{v(t)}{r} - \frac{F_r^r[v](t)(1-r)}{r} \\ &= \frac{v(t)}{r} - \frac{1-r}{r}\min\left\{\frac{v(t)-r}{1-r}, \min\left\{\kappa v(t) + \lambda, w(t_i)\right\}\right\} \quad (t_i < t \le t_{i+1}) \end{aligned} \tag{11}$$

The relationship between LSSO and RSPO, and that between RSSO and LSPO are illustrated in Figure 2. Obviously, as the input varies periodically between 0 and 1, the point of input and output pair, (v, w), moves in the counterclockwise direction

on the RSPOs and LSPOs, but it moves in the clockwise direction on the RSSOs and LSSOs. They are related by the following complementary expressions:

$$rE_r^l[v](t) + (1-r)F_r^l[v](t) = v(t), \tag{12}$$

and

$$rE_r^l[v](t) + (1-r)F_r^l[v](t) = v(t). \tag{13}$$

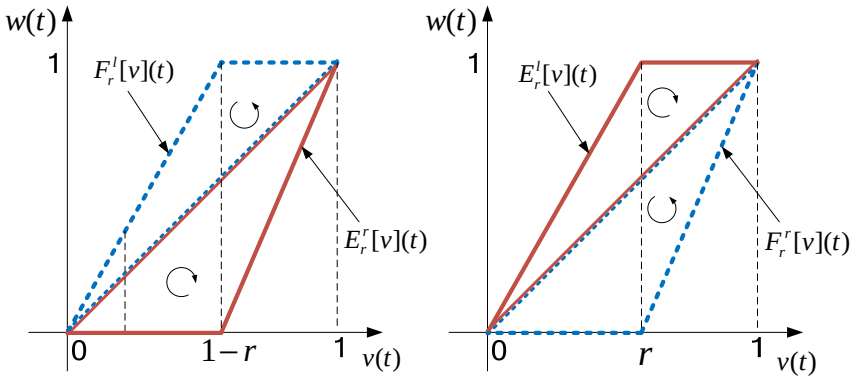

Figure 2: The transfer characteristic of an RSSO and LSSO and their relationship with LSPO and RSPO

The definition of the inverse modified Prandtl-Ishlinskii model is given by

$$z(t) = H^{-1}[x](t) = gv(t) + \int_0^{R'} a^r(r')E'^r_r[x](t)dr' + \int_0^{R'} a^l(r')E'^l_r[x](t)dr', \tag{14}$$

where r' is the threshold of the RSSOs and LSSOs, $a^r(r')$ and $a^l(r')$ are density functions, and R' is the upper limit of r'. g is a constant that satisfies

$$g = \left(1 - \int_0^{R'} a^r(r')dr' - \int_0^{R'} a^l(r')dr'\right) \tag{15}$$

For fast implementation of the inverse modified Prandtl-Ishlinskii model in real-time controllers, an appropriate discrete form is necessary and it can be obtained

by translating the integrations in Eq. (14) to summations, given by

$$\begin{aligned} z(t) = H^{-1}[x](t) &= \left(1 - \sum_{j=1}^{N} a_j^r - \sum_{j=1}^{N} a_j^l\right) x(t) + \sum_{j=1}^{N} a_j^r E_{r_j'}^r[x](t) + \sum_{j=1}^{N} a_j^l E_{r_j'}^l[x](t) \\ &= x(t) + \sum_{j=1}^{N} a_j^r \left(E_{r_j'}^r[x](t) - x(t)\right) + \sum_{j=1}^{N} a_j^l \left(E_{r_j'}^l[x](t) - x(t)\right) \end{aligned} \tag{16}$$

Eq. (16) refers to the discrete expression of the inverse modified Prandtl-Ishlinskii model, which relates the desired displacement x to the compensated voltage z. In order to implement inverse control the parameters a_j^r and a_j^l must be determined from experimental data.

There are two approaches to determine the parameters a_j^r and a_j^l. The first is to caculate the parameters a_j^r and a_j^l from the direct inversion of Eq. (19) by letting $N = M$, the parameters of which can be calculated using a recursive method introduced in [Jiang *et al.* (2009)]. The second is to identify a_j^r and a_j^l directly from experimental data using a recursive method introduced in the next section. The direct inversion of Eq. (19) is introduced in this section.

First, the ascending branch, in which both the normalized input voltage and the normalized output displacement vary from 0 to 1, is considered. Obiously the asceding branch in the direct modified Prandtl- Ishlinskii model and the inverse modified Prandtl- Ishlinskii model can be expressed by

$$x(t) = H[v](t) = v(t) + \sum_{j=1}^{M} q_j^r \left(F_{r_j}^r[v](t) - v(t)\right), \tag{17}$$

$$z(t) = H^{-1}[x](t) = x(t) + \sum_{j=1}^{M} a_j^l \left(E_{r_j'}^l[x](t) - x(t)\right), \tag{18}$$

because $\sum_{j=1}^{M} a_j^r \left(E_{r_j'}^r[x](t) - x(t)\right)$ and $\sum_{j=1}^{M} q_j^l \left(F_{r_j}^l[v](t) - v(t)\right)$ are zero on the asceding branch. The corresponding values of the threshold r_j are supposed to be r_j'. Obviousy,

$$r_j' = r_j + \sum_{j=1}^{M} q_j^r \left(f_{r_j}^r(r_j, 0, 1, 0) - r_j\right), \tag{19}$$

Corresponding to Eqs. (20) and (21), two functions $\varphi(v)$ and $\psi(x)$ are defined as

follows:

$$\varphi(v) = v + \sum_{j=1}^{M} q_j^r \left(f_{r_j}^r (v,0,1,0) - v \right), \tag{20}$$

$$\psi(x) = x + \sum_{j=1}^{M} a_j^l \frac{1-r_j'}{r_j'} \left(x - f_{r_j'}^r (x,0,1,0) \right). \tag{21}$$

Obviously, $\psi(x)$ is the inverse function of $\varphi(v)$. Their derivatives, $\varphi'(v)$ and $\psi'(x)$, are

$$\varphi'(v) = 1 - \sum_{j=J}^{M} q_j^r, \tag{22}$$

$$\psi'(x) = 1 - \sum_{j=J}^{M} a_j^l \frac{1-r_j'}{r_j'}, \tag{23}$$

for $r_{j-1} < v < r_j$ and $r'_{j-1} < x < r'_j (j = 1, \cdots, M)$. It is assumed that $r_0 = r'_0 = 0$ and $r_{M+1} = r'_{M+1} = 1$. Obviously, $\varphi'(v)$ and $\psi'(x)$are piece-wise constant functions. Since $\psi(x)$ is the inverse function of $\varphi(v)$, there exists

$$\psi'(x) = \left(\varphi'(v) \right)^{-1}. \tag{24}$$

The a_j^r can be solved from Eqs. (22)-(23) by changing j from M to 1. In the same way, the parameters a_j^l can also be obtained.

2.3 The parameter identification of inverse model

The parameters a_j^r and a_j^l can also be identified directly from experimental using a recursive approach. Suppose the measurement data in the physical system are

$$\{(\tilde{v}_1, \tilde{x}_1), (\tilde{v}_2, \tilde{x}_2), \cdots, (\tilde{v}_k, \tilde{x}_k), \cdots, (\tilde{v}_K, \tilde{x}_K)\}. \tag{25}$$

The measurement data can not be used directly for model identification as the input and output variables associated with the model are constrained to the unity range, so that the measurement data should be transformed to that range through a normalization process. Assume corresponding input and output data in the model space are

$$\{(v_1, x_1 = H[v_1]), (v_2, x_2 = H[v_2]), \cdots, (v_k, x_k = H[v_k]), \cdots, (v_K, x_K = H[v_K])\}, \tag{26}$$

the transformation rule of data from physical space to the model space is given by

$$v_k = \frac{\tilde{v}_k - \tilde{v}_{\min}}{\tilde{v}_{\max} - \tilde{v}_{\min}}, \quad x_k = \frac{\tilde{x}_k - \tilde{x}_{\min}}{\tilde{x}_{\max} - \tilde{x}_{\min}}, \tag{27}$$

where

$$\begin{aligned} &\tilde{v}_{\max} = \max\{\tilde{v}_1, \tilde{v}_2, \cdots, \tilde{v}_K\},\ \tilde{v}_{\min} = \min\{\tilde{v}_1, \tilde{v}_2, \cdots, \tilde{v}_K\}, \\ &\tilde{x}_{\max} = \max\{\tilde{x}_1, \tilde{x}_2, \cdots, \tilde{x}_K\},\ \tilde{x}_{\min} = \min\{\tilde{x}_1, \tilde{x}_2, \cdots, \tilde{x}_K\}. \end{aligned} \tag{28}$$

The approach for parameter identification is basically a recursive least-square algorithm and the updating expressions are given by

$$\begin{aligned} \mathbf{a}^r(k+1) &= \mathbf{a}^r(k) + 2\gamma e(k)\left[\mathbf{E}^r[x(k)] - \mathbf{x}(k)\right], \\ \mathbf{a}^l(k+1) &= \mathbf{a}^l(k) + 2\gamma e(k)\left[\mathbf{E}^l[x(k)] - \mathbf{x}(k)\right], \end{aligned} \tag{29}$$

where

$$\begin{aligned} e(k) = e_k &= V_{ck} - \left(x_k + \sum_{j=1}^{M} a_j^r \left(E_{r_j}^r[x_k] - x_k \right) + \sum_{j=1}^{M} a_j^l \left(E_{r_j}^l[x_k] - x_k \right) \right) \\ \mathbf{a}^r &= [a_1^r, a_2^r, \cdots, a_M^r],\ \mathbf{a}^l = [a_1^l, a_2^l, \cdots, a_M^l], \\ \mathbf{E}^r[x(k)] &= \mathbf{E}^r[x_k] = \left[E_{r_1'}^r[x_k], E_{r_2'}^r[x_k], \cdots, E_{r_M'}^r[x_k] \right], \\ \mathbf{E}^l[x(k)] &= \mathbf{E}^l[x_k] = \left[E_{r_1'}^l[x_k], E_{r_2'}^l[x_k], \cdots, E_{r_M'}^l[x_k] \right], \\ \mathbf{x}(k) &= \mathbf{x}_k = [x_k, x_k, \cdots, x_k]_{1\times M}. \end{aligned} \tag{30}$$

Here k is the number of iteration, $V_{ck} = V_c(k)$ is compensated command voltage as discussed later, x_k is the measured displacement, and γ is the iteration gain which determines the learning rate of the identification. The recursion law shown in Eq. (30) guarantees that the normalized error tends to zero asymptotically [Narendra and Annaswamy (1989)]. In real-time control applications, the value 0.1 for γ is enough to guarantee the inverse hysteresis model converges rapidly. The convergence criterion of the inverse hysteresis model is defined as that $|e_k - e_{k-1}|$ is smaller than a certain value.

The parameters $\mathbf{a}^r$ and $\mathbf{a}^l$ have initial values for the first recursion. Theoretically the initial values can be arbitrary, but normally zero vectors were used as their initial value. Using one experimental data set, the identification procedure shown in Eq. (30) can be repeated for several times until satisfactory results are obtained. However, the identified values of $\mathbf{a}^r$ and $\mathbf{a}^l$ in the previous experiment can be used

as the initial value in the next experiment. The parameter identification procedure can be also expressed in signal flow chart form, which is shown in Fig. 3.

As soon as the model identification is completed, the model can be implemented to generate output data from input data, and input and output data obtained in the model space should be re-transfered to their original physical space. The transformation rules from model space to the physical space are given by

$$\tilde{v}_k = v_k(\tilde{v}_{\max} - \tilde{v}_{\min}) + \tilde{v}_{\min} \tag{31}$$

$$\tilde{x}_k = y_k(\tilde{x}_{\max} - \tilde{x}_{\min}) + \tilde{x}_{\min} \tag{32}$$

3 Inverse Controllers and Experimental System

In this study, hysteresis compensation of the piezoelectric actuator is performed with an inverse control system. The system block diagram is given by Fig. 4, where $\tilde{x}_r$ is the command displacement, and x_r is the normalized command displacement. $\tilde{V}_r$ is uncompensated driving voltage corresponding to $\tilde{x}_r$ and V_r is its normalized form. $\tilde{x}_r$ and $\tilde{V}_r$are proportional with their ratio equal to the sensitivity of the piezoelectric actuator, but due to normalization, $x_r = V_r$. The inverse controller transfers the driving voltage from x_r or V_r to a compensated voltage V_c, which is then amplified to drive the piezoelectric actuator. The inverse controller utilizes the proposed inverse model shown in Eq. (16) for the inverse compensation of V_r. The uncompensated voltage V_r and the compensated voltage V_c correspond to the input $x(t)$ and output $z(t)$ of the inverse operator in Eq. (16), respectively. The hysteresis identifier is used to generate parameters for the inverse model of piezoelectric actuators. The thresholds r'_j of the RSSOs and LSSOs in the inverse model are determined by $r'_j = j/(M+1)$ $(j = 1, \cdots, M)$. The number of RSSOs and LSSOs, M, was set to 19 in the control experiments.

The switch in Fig. 4 can change the operation mode of the control system. When it is turned off, the parameters in the inverse controller are fixed and the controller is just a feedforward inverse controller; but when it is turned on, the parameters in the inverse controller is updated in each time step by the hysteresis identifier and the controller becomes an adaptive inverse controller. In the turned-off mode, the identified parameters are copied to the inverse controller from the hysteresis identifier once the inverse hysteresis model converged, and the driving voltage is compensated to guarantee that the output displacement of the piezoelectric actuator is equal to the command displacement x_r or proportional to the uncompensated driving voltage V_r.

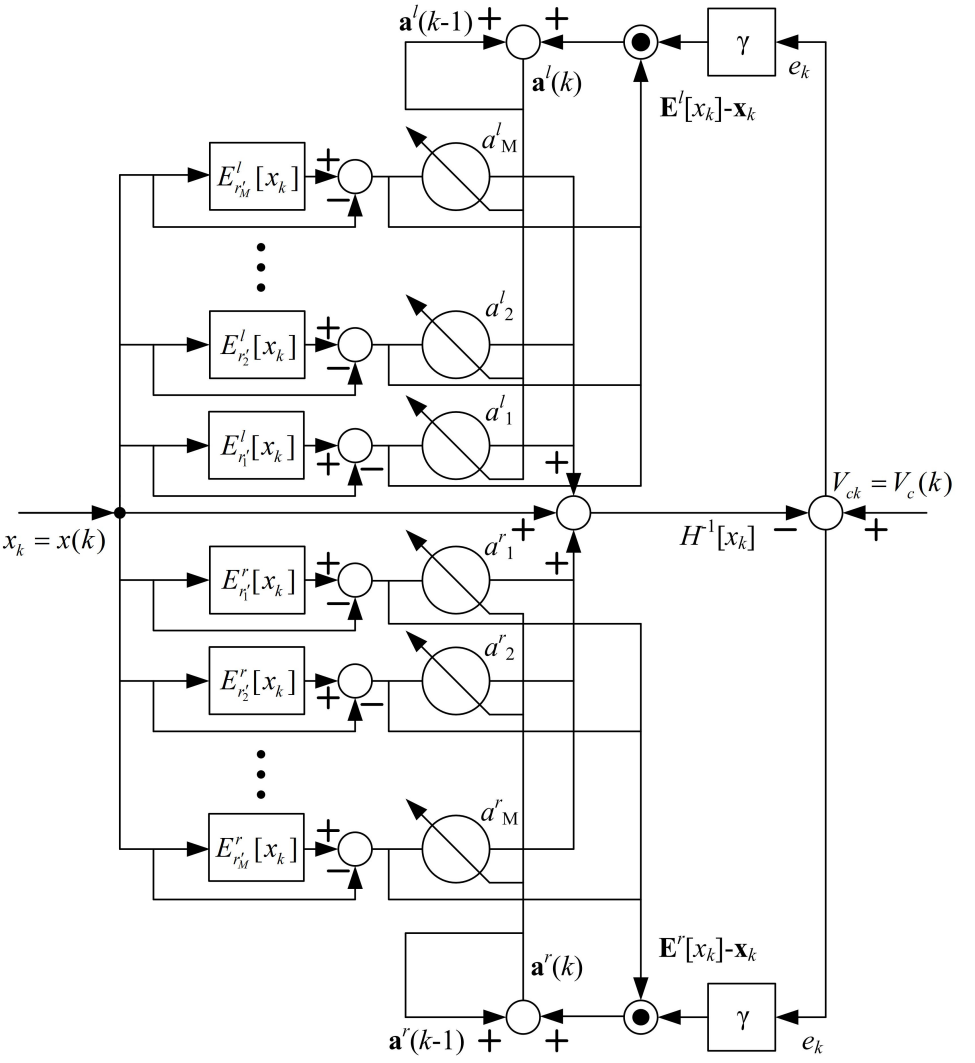

Figure 3: The signal flow chart of the hysteresis identifier

The experimental setup is shown in figure 5. The setup includes a dSPACE board hosted by a personal computer, a power amplifier, a fiber sensor and a piezoelectric stack actuator. The host computer was used to generate the control codes, which were downloaded and implemented in dSPACE control board. The power amplifier was used to amplify the voltage to the piezoelectric stack actuators. The displacements of the actuator were measured with a fiber sensor. All measurement data were sent to the host computer and saved.

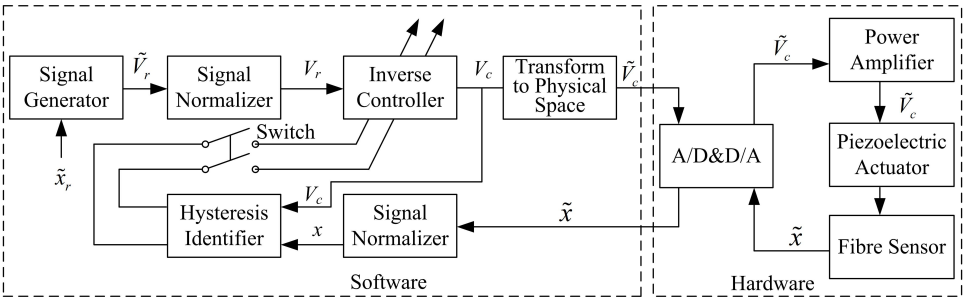

Figure 4: The block diagram of the inverse control system

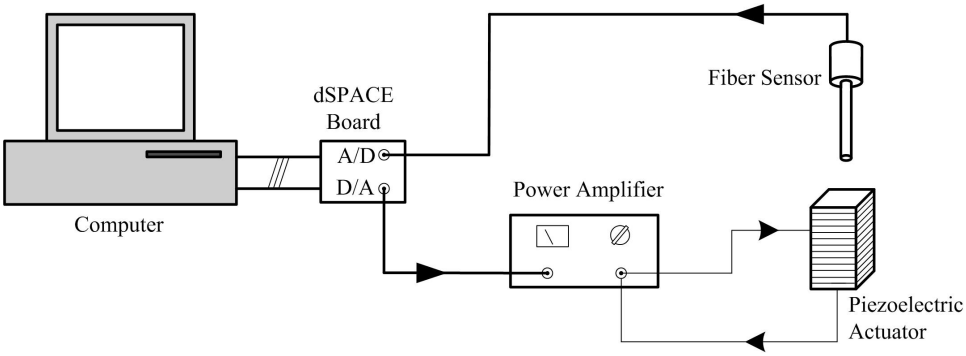

Figure 5: The experimental setup

4 Experimental Results and Discussion

The first experiment performs feedforward inverse control to the piezoelectric actuator in tracking 0.5Hz sinusoidal driving voltage with varying amplitudes. Figure 6(a) illustrates the uncompensated voltage and the compensated voltage signals. Figure 6(b) shows the measured displacement and Fig. 6(c) shows the measured displacement versus uncompensated driving voltage. Figures 7 and 8 show the experimental results where the driving voltage waveforms are different. It's clear that in the above three conditions the measured displacement is almost exactly proportional to the uncompensated driving voltage, and further analysis indicates that hysteresis nonlinear errors between the uncompensated driving voltage and the measured displacement in the three conditions are reduced to lower than 1.87%, 2.17% and 2.31% of the total displacement range respectively.

The second experiment performs adaptive inverse control to the piezoelectric actuator under the same driving voltage conditions as used in the first experiment. The graphical results are shown in Figs. 9-11 respectively. The presence of adap-

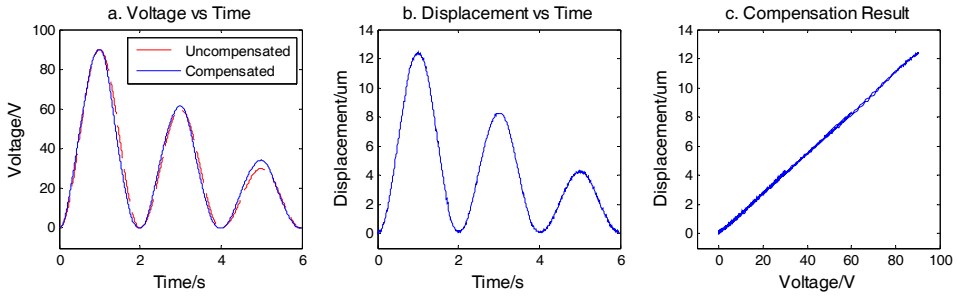

Figure 6: Hysteresis compensation with feedforward inverse controller: the first case

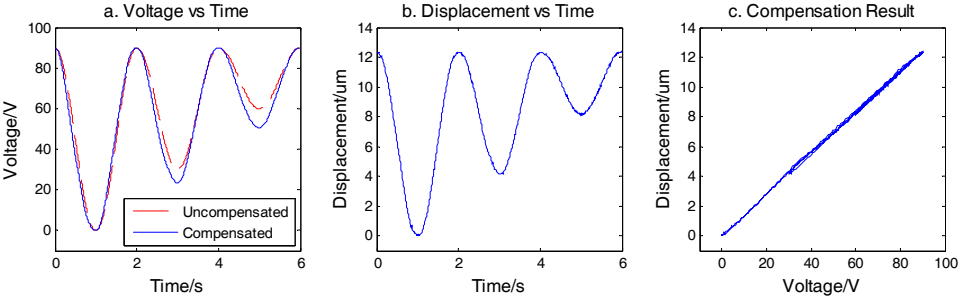

Figure 7: Hysteresis compensation with feedforward inverse controller: the second case

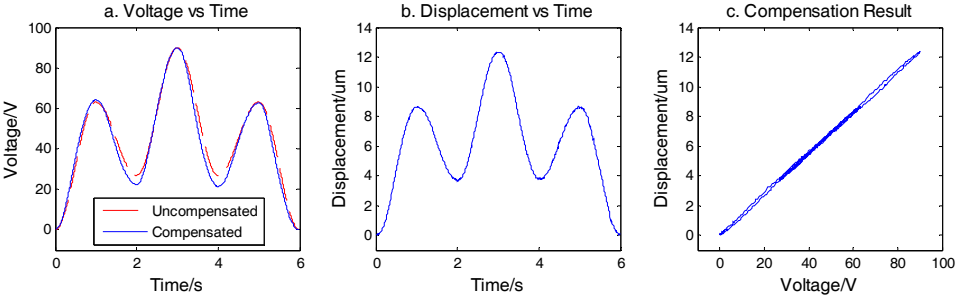

Figure 8: Hysteresis compensation with feedforward inverse controller: the third case

tive inverse controller can slightly raise the performance of the control system. The hysteresis nonlinear errors between the uncompensated driving voltage and the measured displacement are depressed to lower than 1.49%, 1.86% and 2.02% of the total displacement range respectively.

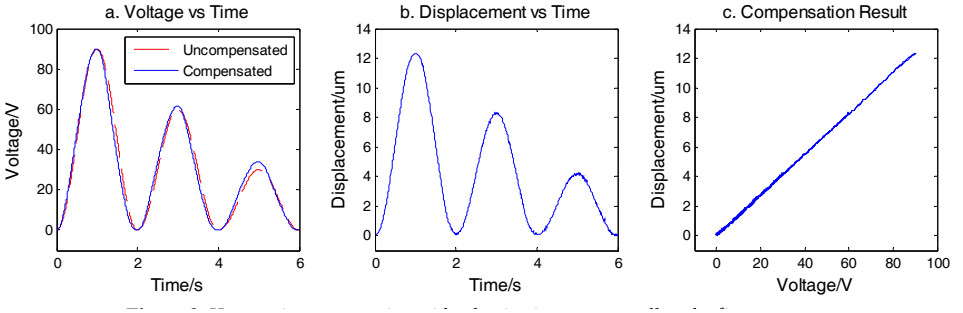

Figure 9: Hysteresis compensation with adaptive inverse controller: the first case

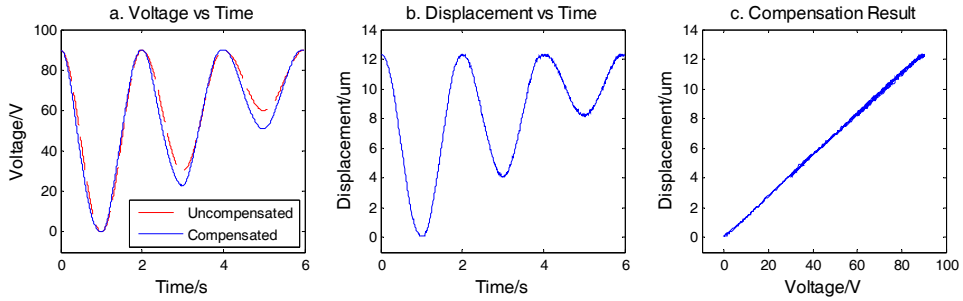

Figure 10: Hysteresis compensation with adaptive inverse controller: the second case

In the above two experiments, the control system operated in two different modes. The main difference between the two modes is association of the adapting ability. The feedforward inverse controller utilizes a fixed inverse model so that the system is highly stable and immune to any disturbance, but in conditions that the hysteresis characteristics are changing with time, the feedforward inverse controller can not adapt to the changes of hysteresis property. The adaptive inverse controller can adapt itself to the changing behavior of the piezoelectric actuators and has exhibited better control performances in the experiment of this study. However, the system is not as stable as the former one. The stability of adaptive control system can be

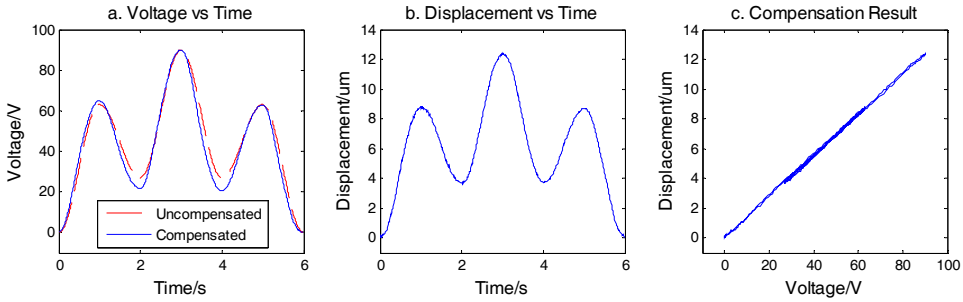

Figure 11: Hysteresis compensation with adaptive inverse controller: the third case

improved by adjusting the convergence coefficient γ online. In real-time control conditions, as disturbances and noise always exist and the hysteresis characteristics of piezoelectric actuators are normally time-invariant, the feedforward inverse controller is more suitable for industry applications.

5 Conclusions

In this study, right-side stop operators (RSSOs) and left-side stop operators (LSSOs) were defined and the inverse modified Prandtl-Ishlinskii model were constructed from the RSSOs and LSSOs for the inverse control of a piezoelectric hysteresis. The proposed inverse model successfully simulated the inverse asymmetric hysteresis loops of the studied piezoelectric actuator. Control system based on the proposed inverse model was designed to operate at two modes: feedforward inverse controller mode and adaptive inverse controller mode. The main advantage of the proposed control system is that the parameters identification procedure can be processed automatically, so it doesn't need to identify the model parameters beforehand. Experiments have been performed on the studied piezoelectric actuator and the results have shown that the control system can significantly reduce the hysteresis nonlinear error of the studied piezoelectric actuator.

Acknowledgement: This research is supported by the Funds for Creative Scholars in "Climbing" Program of Jiangsu province (Grant No.BK2009020), the Major Research plan of the National Natural Science Foundation of China (Grant No.90923029), the Program for Changjiang Scholars and Innovative Research Team in University (IRT0968), and the Priority Academic Program Development of Jiangsu Higher Education Institutions.

References

Ang, W. T.; Riviere, C. N.; Khosla, P. K. (2007): Feedforward controller with inverse rate-dependent model for piezoelectric actuators in trajectory-tracking applications. *IEEE-ASME T. Mech.,* vol. 12, pp. 134-142.

Badel, A.; Qiu, J. H.; Sebald, G.; Guyomar, D. (2007): Self-sensing High Speed Controller for Piezoelectric Actuator. *J. Intell. Mater. Syst. Struct.,* vol. 19, pp. 395-405.

Barrett, R. C.; Quate, C. F. (1991): Optical scan-correction system applied to atomic force microscopy, *Rev. Sci. Instrum.*, vol. 62, pp. 1393-1399.

Brokate, M.; and Kenmochi, N. (1996): *Hysteresis and Phase Transitions*, Berlin, Ger: Springer-Verlag.

Croft, D.; Stilson, S.; Devasia, S. (1999): Optimal tracking of piezo-based nanopositioners. *Nanotechnology*, vol. 10, pp. 201-208.

Furutani, K.; Urushibata, M.; Mohri, N. (1998): Displacement control of piezoelectric element by feedback of induced charge. *Nanotechnology*, vol. 9, pp. 93-98.

Ge, P.; Jouaneh, M. (1995): Modeling hysteresis in piezoceramic actuators. *Prec. Eng.*, vol. 17, pp. 211-221.

Ge, P., Jouaneh, M. (1996): Tracking control of a piezoceramic actuator. *IEEE Trans. Control Syst.,* vol. 4, pp. 209-216.

Goldfarb, M.; Celanovic, N. (1997): Modeling piezoelectric stack actuators for control of micromanipulation. *IEEE Contr. Mag.*, vol. 17, pp. 69-79.

Hughes, D.; Wen, J. T. (1997): Preisach modeling of piezoceramic and shape memory alloy hysteresis. *Smart Mater. Struct.*, vol. 6, pp. 287-300.

Hu, H.; Mrad, R. B. (2002): On the classical Preisach model for hysteresis in piezoceramic actuators. *Mechatronics*, vol. 13, pp. 85-94.

Janocha, H.; Kuhnen, K. (2000): Real-time compensation of hysteresis and creep in piezoelectric actuators. *Sens. Actuators, A*: *Physical*, vol. 79, pp. 83-89.

Janaideh, M. Al.; Su, C. Y.; Rakheja, S. (2008): Development of the rate-dependent Prandtl-Ishlinskii model for smart actuators. *Smart Mater. Struct.*, vol. 17, pp. 1-11.

Jiang, H.; Ji, H. L.; Qiu, J. H.; Chen, Y. S. (2009): A Modified Prandtl-Ishlinskii Model for Modeling Asymmetric Hysteresis of Piezoelectric Actuators. *IEEE T Ultrason. Ferr.*, vol. 57, 1200-1210.

Kuhnen, K. (2003): Modeling, identification and compensation of complex hysteretic nonlinearities. *Eur. J. Control,* vol. 9, pp. 407-418.

Miller, R. C.; Savage, A. (1959): Asymmetric Hysteresis Loops and the Pyroelec-

tric Effect in Barium Titanate. *J. Appl. Phys.*, vol. 30, pp. 808-811.

Narendra, K. S.; Annaswamy, A. M. (1989): *Stable Adaptive Systems*, Englewood Cliffs, NJ: Prentice-Hall.

Newcomb, C. V.; Flinn, I. (1982): Improving the linearity of piezoelectric ceramic actuators. *Electron. Lett.*, vol. 18, pp. 442-444.